TENSILE TESTING OF UNIDIRECTIONAL SILICON CARBIDE COMPOSITES FOR FUTURE IRRADIATION EXPERMENTS

T. Hinoki[1], L.L. Snead[2], E. Lara-Curzio[2], Y. Katoh[1] and A. Kohyama[1]
(1) Institute of Advanced Energy, Kyoto University); (2) Oak Ridge National Laboratory

OBJECTIVE

The objective of this study is, to develop the experimental method of tensile tests of the SiC/SiC composites to be irradiated, and to obtain tensile properties of the unirradiated SiC/SiC composites expected for fusion application.

SUMMARY

The SiC/SiC composites, which have three kinds of unidirectional stoichiometric SiC fibers and various fiber coating, were prepared by I-CVI method for future irradiation experiments. In-plane tensile bars and transthickness tensile specimens were cut from these materials. In-plane tensile tests, transthickness tensile tests and four point bend tests were carried out at ambient temperature. While the specimens, SCS-9A™ fibers were used, showed superior ultimate tensile stress, more than 1 GPa, to the other specimens, proportional limit stress of the specimens, Hi-Nicalon™ type-S fibers were used, was larger than the other specimens. The specimens, Tyranno™ SA fibers were used or multiple SiC fiber coating was applied, showed brittle fracture behavior. Correlation between tensile results and flexural results was discussed. Transthickness tensile tests were unsuccessful because of insufficient bond between fixture and epoxy.

PROGRESS AND STATUS

1. INTRODUCTION

The high temperature mechanical properties and low activation make SiC/SiC composites very attractive as fission and fusion reactor materials [1]. At present, interfacial properties between the fiber and matrix of neutron-irradiated SiC/SiC composites limit mechanical performance [2]. This limitation has been attributed primarily to shrinkage in the SiC-based fibers due to irradiation-assisted oxidation [3], irradiation-induced recrystalization of microcrystalline fibers [4-6], and to large dimensional changes of the carbon [7] coating applied to the fiber. To avoid or at least minimize these radiation effects, the recent trend in SiC fiber development is toward lower oxygen content, reduced free carbon and enhanced crystallinity. Previous work regarding ion-irradiation

effect on carbon interphase microstructure indicated that the basal planes of the irradiated graphite-like carbon appear to be chopped into small fragments and consequently amorphous-like structures were observed [8]. The development of more radiation-resistant SiC composites is based on the use of stoichiometric SiC fibers with lower oxygen and SiC-based coating. Recently, stoichiometric SiC fibers have been developed including Hi-Nicalon™ type-S [9], Sylramic™, Tyranno™ SA [10] and SCS-9A™ [11].

It was difficult to evaluate actual mechanical performance of SiC/SiC composites by flexural tests. Flexural strength includes tensile strength, compression strength and interfacial shear strength. This difficulty attributes to mismatch of tensile strength and compression strength of SiC/SiC composites. To appreciate mechanical performance of SiC/SiC composites, evaluation by tensile tests are desired rather than flexural tests. However tensile testing of SiC/SiC composites is more difficult than the other materials due to limitation of size and difficulty of processing. In this study, tensile tests of the SiC/SiC composites with stoichiometric fibers and various interphase to be irradiated was successfully carried out.

2. EXPERIMENTAL

Materials

The materials used in this study were unidirectional SiC fiber reinforced SiC composites and fabricated by isothermal chemical vapor infiltration (I-CVI) method at Hyper-Therm High-Temperature Composites, Inc. for ORNL/Kyoto University round robin irradiation program. All fibers used were low oxygen stoichiometric SiC fiber, Hi-Nicalon™ type-S, Tyranno™ SA and SCS-9A™, while SCS-9A™ has a carbon core 33 μm in diameter and outer silicon-rich carbon layers [12]. Fiber properties were reported as shown in Table 1 [9-11]. Fibers were coated with either carbon, multiple SiC or "porous" SiC by CVI prior to matrix deposition. Mixtures of methyltrichlorosilane, argon, methane and hydrogen gases were used to deposit the "porous" SiC coating on fiber. In the multiple SiC interphase, the first SiC layer was deposited followed by a thin,

Table 1: The properties of stoichiometric SiC fibers used in this work

SiC Fiber	C/Si Atomic Ratio	Oxygen Content (wt%)	Tensile Strength (GPa)	Tensile Modulus (GPa)	Elongation (%)	Density (g/cm³)	Diameter (?m)
Hi-Nicalon Type-S	1.05	0.2	2.6	420	0.6	3.10	12
Tyranno SA	1.08	0.3	2.8	420	0.7	3.02	10
SCS-9A	1.0	0	3.45	307	1.1	2.8	79

interrupted layer of pyrolytic carbon. Four SiC layers were fabricated with interrupted pyrolytic carbon in the multiple SiC coating [13]. Properties of the SiC/SiC composites used are shown in Table 2. SEM images of cross section of the specimens with C fiber coating were shown in Fig. 1, respectively. Fiber coating thickness and fiber volume fraction was estimated from SEM images of cross section. One of the reasons for low fiber volume fraction was extra SiC coating of the SiC/SiC composites as seal coating.

Technique

Two kinds of tensile tests were carried out. One was standard tensile test for fiber direction, in-plane tensile test. For this, the specimens with straight-gauge section were prepared. The specimen size was 50^{l} x 4^{w} x 1.5^{t} mm for Hi-Nicalon^{TM} type-S samples and Tyranno^{TM} SA specimens or 50^{l} x 4^{w} x 1.0^{t} mm for SCS-9A^{TM} specimens. These specimens had 18^{l} x 4^{w} x 1.5^{t} mm and 18^{l} x 4^{w} x 1.0^{t} mm gauge size, respectively. Wedge-type grip was used. Aluminum tabs were applied between specimens and grip to adjust the specimens to grip and to promote uniform stress within grip. Aluminum tab surfaces were serrated by a rough file and attached to specimens by the epoxy to prevent slippage between an aluminum tab and a specimen. A specimen with aluminum tabs was fixed in the couple of fixtures with sufficient lateral pressure to prevent slippage between the fixture and a specimen. This specimen with the fixture was fixed to the load train couplers. The load train couplers

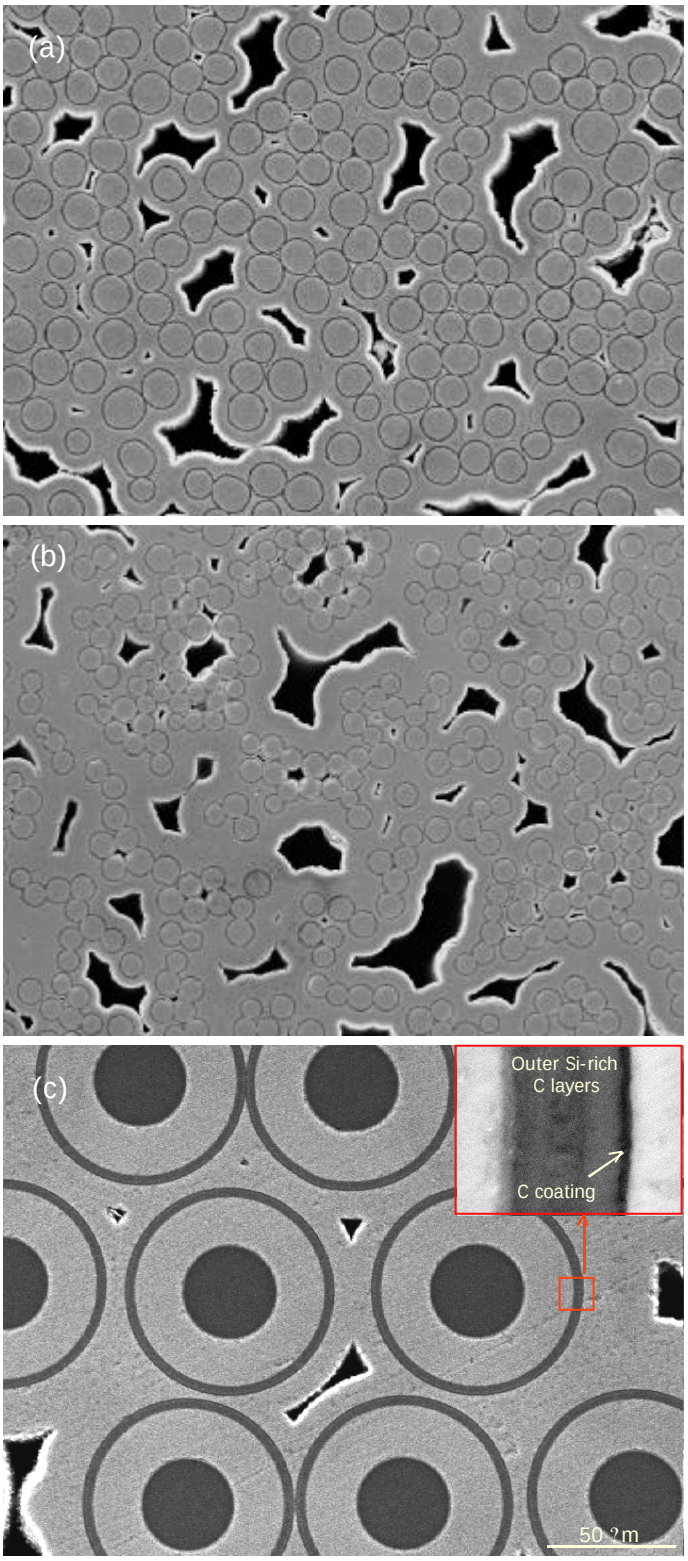

Fig. 1: SEM images of cross section of the specimens with C fiber coating, (a) Hi-Nicalon^{TM} type-S, (b) Tyranno^{TM} SA and (c) SCS-9A^{TM} specimen

Table 2: Properties of the specimens

ID	TST1	TST2	TSM	TSP	SAC	SAM	S9C	S9M	S9P
Fiber	Hi-Nicalon™ Type-S				Tyranno™ SA		SCS-9A™		
Fiber Coating	C		Multiple SiC	"Porous" SiC	C	Multiple SiC	C	Multiple SiC	"Porous" SiC
Coating Thickness (nm)	520	720	580	380	560	880	330	580	240
Density (g/cm^3)	2.58	2.58	2.65	2.56	2.55	2.53	2.64	2.60	2.56
Vf (%)	29	29	38	26	21	24	32	33	38

was non fixed load train couplers with universal joints, which promote self-alignment of the load train during the movement of crosshead to reduce specimen bend. The fixture and the load train couplers are based on ASTM C1275. A specimen, the fixture and the load train coupler are shown in Fig. 2. The strain was measured by means of the capacitive extensometer (Instron Inc.). Two balanced arms, pivoted in the center, transmit the displacement of the specimen to an outboard capacitive transducer to measure the specimen strain. However the distance of these two arms was 25 mm, while gauge length of the specimens was 18 mm. The supplementary arms to measure this shorter gauge was prepared and fixed to original arms. The capacitive extensometer with the supplementary arms was shown in Fig. 3. All tests were conducted with the cross-head speed of 10 µm/sec at ambient temperature.

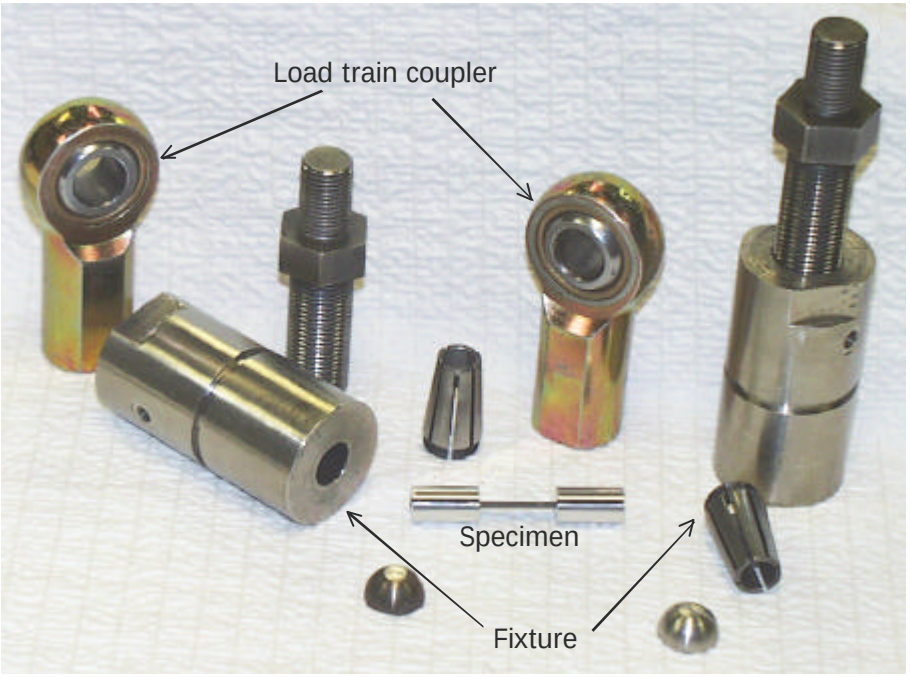

Fig. 2: Specimen, fixture and load train coupler for in-plane tensile test

Four point bend tests were carried out to correlate with tensile properties. The same specimens with in-plane tensile specimens

were used. The support span and the load span were 40 mm and 20 mm, respectively. The crosshead speed was 0.021 mm/sec.

Transthickness tensile tests were also carried out to evaluate shear stress of fracture mode I. The specimens, whose size were 5^{l} x 5^{w} x 1.5^{t} mm for Hi-Nicalon^{TM} type-S specimens and Tyranno^{TM} SA specimens or 5^{l} x 5^{w} x 1.0^{t} mm for SCS-9A^{TM} specimens, were prepared. The pair of fixtures, which have 5 mm square face to attach the specimen, were also prepared. The fixture attached to the specimen by the epoxy was connected to the load train couplers, which have universal joints to promote self-alignment of the load train during the movement of crosshead to reduce specimen bend. The specimens, the fixtures and the load train couplers are shown in Fig. 4. All tests were conducted with the cross-head speed of 10 μm/sec at ambient temperature.

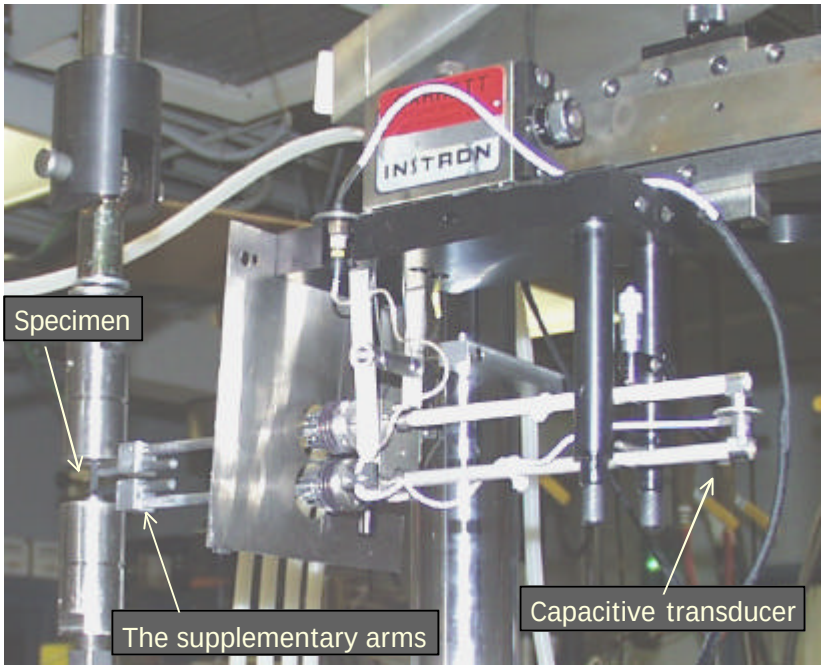

Fig. 3: Capacitive transducer with the supplementary arms

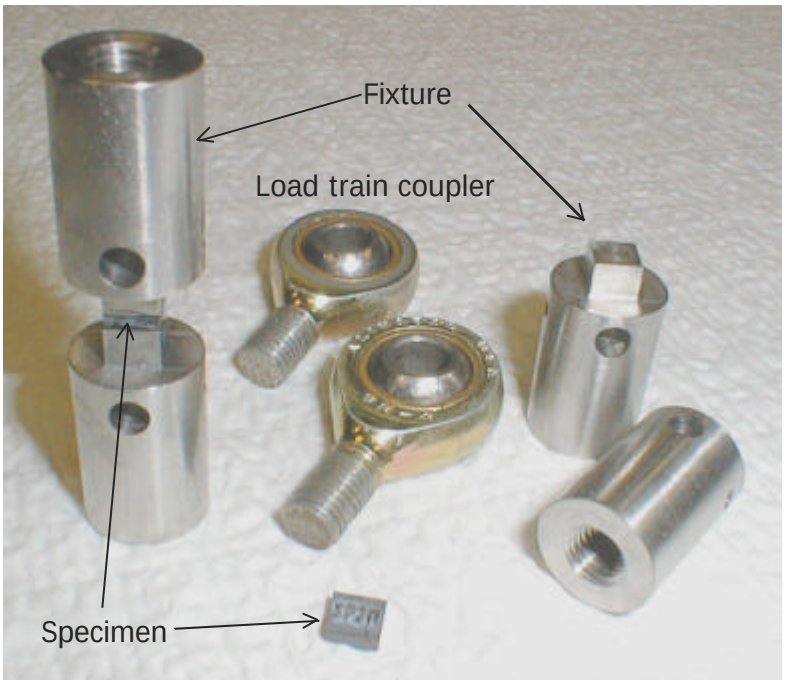

Fig. 4: Specimen, fixture and load train coupler for transthickness tensile test

3. Results

In-plain tensile tests

Stress-strain behavior of three specimens, which have Hi-Nicalon^{TM} type-S, Tyranno^{TM} SA and SCS-9A^{TM}, respectively, and C interphase between fiber and matrix, are shown in Fig. 5. This shows the typical effect of fiber properties on mechanical properties and trend of whole results. SCS-9A^{TM} specimens showed larger average ultimate tensile stress (UTS) and strain than Hi-Nicalon^{TM} type-S specimens and Tyranno^{TM} SA specimens, while proportional limit stress (PLS) of Hi-Nicalon^{TM} type-S

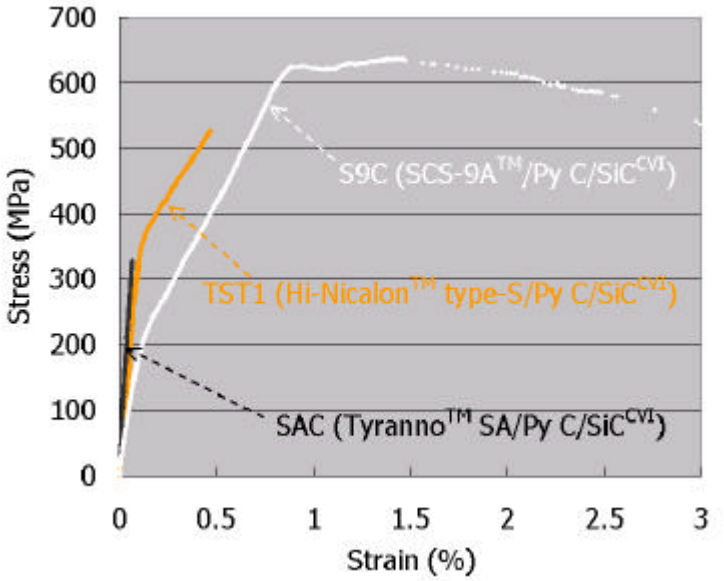

Fig. 5: Effect of fiber properties on strain-stress curve of tensile tests

specimens was largest. PLS was obtained from 0.01 % strain offset. Average modulus of Tyranno™ SA specimens was larger than the others. These tensile properties corresponded to fracture surfaces in Fig. 6. A few mm fiber pullouts are shown in SCS-9A™ specimens fracture surface. TST1 specimens showed fiber pullouts in a little complicated fracture surface compared to SAC specimens. SAC specimens showed very brittle fracture behavior.

Tensile properties and fracture behaviors were affected by fiber coating, respectively. Multiples coating specimens showed smaller UTS than the other coating specimens. PLS and modulus of multiple coating specimens were also smaller in Hi-Nicalon™ type-S specimens and Tyranno™ SA specimens. Multiple SiC coating specimens were brittle compared to the other coating specimens. “Porous” SiC coating specimens of SCS-9A™ specimens showed better tensile properties than C coating specimens, although C coating specimens were better in Hi-Nicalon™ type-S specimens. The results of these tensile tests are summarized in table 3.

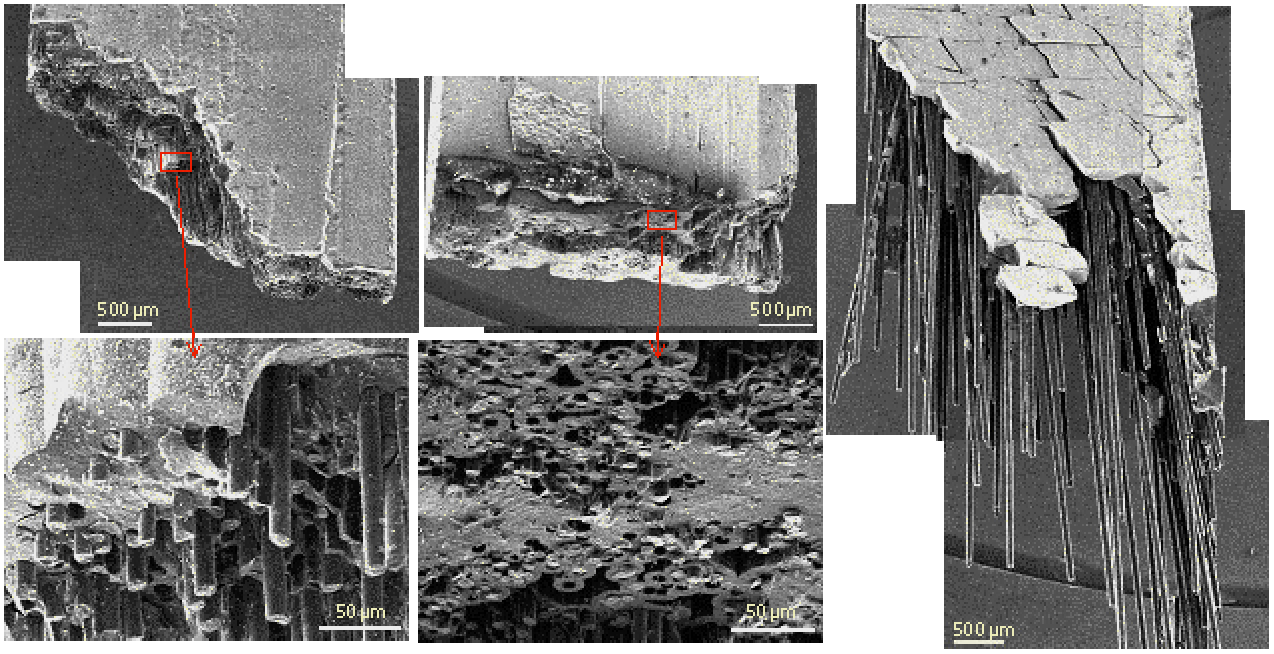

Fig. 6: Effect of fiber properties on fracture surface after tensile tests

Table 3: Summary of mechanical properties

ID	TST1	TST2	TSM	TSP	SAC	SAM	S9C	S9M	S9P
Tensile Modulus (GPa)	336	306	256	307	417	350	203	294	373
Flexural Modulus (GPa)	296	284	237	260	219	205	347	302	350
Tensile PLS (MPa)	339	268	229	276	220	148	166	246	227
Flexural PLS (MPa)	490	533	356	422	214	199	260	321	356
UTS (MPa)	442	319	229	282	220	148	622	562	860
Flexural Strength (MPa)	907	748	757	485	255	199	982	908	959

Four point bend tests

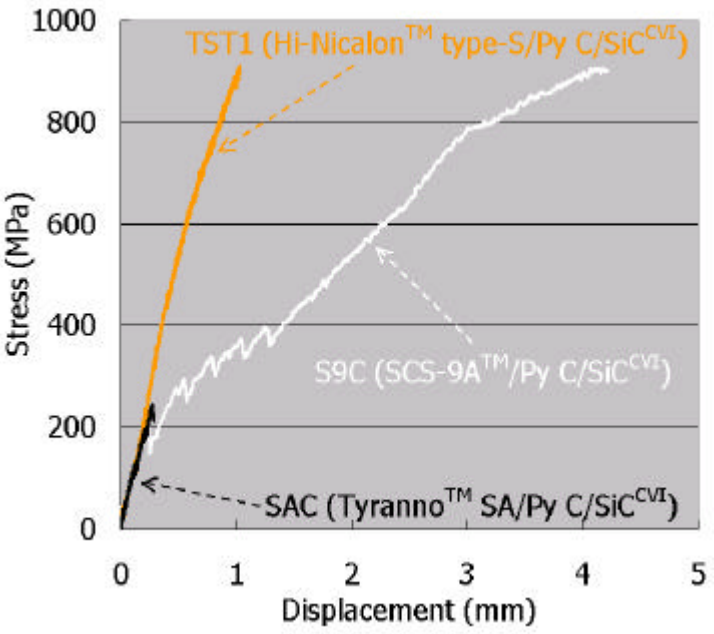

Fig. 7: Effect of fiber properties on flexural

Flexural stress and PLS showed similar trend to tensile results. Flexural curve of three specimens, which have Hi-Nicalon™ type-S, Tyranno™ SA and SCS-9A™, respectively, and C interphase between fiber and matrix, are shown in Fig. 7. SCS-9A™ specimens showed larger flexural stress and strain than Hi-Nicalon™ type-S specimens and Tyranno™ SA specimens, while PLS of Hi-Nicalon™ type-S specimens was largest. PLS was obtained from 0.01 % strain offset. However modulus of Tyranno™ SA specimens was not largest but smallest. PLS and flexural stress of four point bend tests were larger than PLS and UTS of tensile tests, especially Hi-Nicalon™ type-S specimens.

There was some different effect of fiber coating on mechanical properties between tensile properties and flexural properties. While multiple SiC fiber coating specimens showed inferior tensile properties to the other fiber coating specimens, they showed some superior properties than the other specimens in flexural tests. Flexural strength of C fiber coating specimens was larger than the other

coating specimens. The results of these flexural tests are also summarized in table 3.

Transthickness tensile tests

All specimens tested were not broken within specimens, but at interface between a specimen and a fixture as shown in Fig. 8. This is because bond between stainless steel and the epoxy was insufficient. Both specimens and fixtures were cleaned well. However all tests were unsuccessful with maximum stress, about 10 MPa.

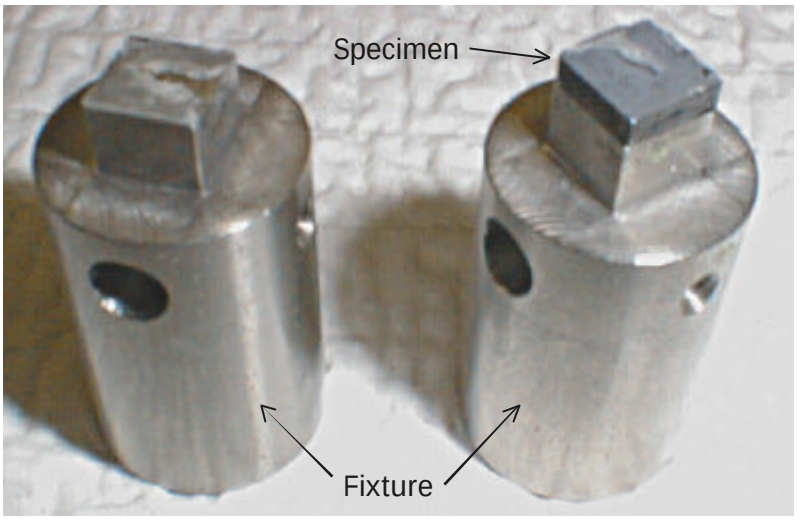

Fig. 8: Specimen and fixture after transthickness tensile test

4. Discussions

Evaluation of Tensile Properties

There was large effect of the fiber on tensile properties. Tyranno™ SA specimens showed very brittle fracture behavior. This is considered that large interfacial shear strength was most of the reasons, while interfacial shear properties were not evaluated yet. Same kind of coating was applied to each fiber. However fiber surface roughness was different, respectively. Interfacial shear properties were different, if a kind of fibers was different. Interfacial coating properties of each fiber should be optimized.

Multiple SiC fiber coating specimens showed relatively brittle fracture behavior. Some papers say that interfacial shear strength of C fiber coating specimens depends on its coating thickness [14,15]. In multiple SiC coating, C coating was just used to interrupt SiC coating and its thickness was very thin. So this interfacial shear strength might be very

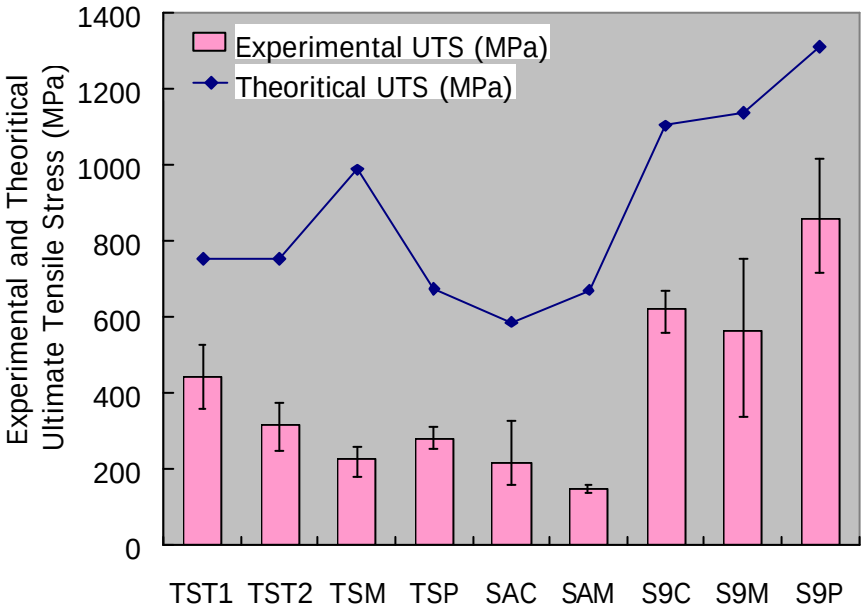

Fig. 9: Comparison of experimental UTS and theoretical UTS

strong. However the specimens used in this work were for neutron irradiation. This multiple coating specimens are expected to show superior properties under neutron irradiation.

Some reasons were inferred regarding relatively low PLS of SCS-9A™ specimens. If the Poison ratio of the fiber is same and there is a gap of the ratio between the fiber and the matrix, the larger fiber diameter specimens is easier to debond at fiber-matrix interface than the smaller diameter fiber specimens.

It is said that UTS depends on fiber strength [16]. Theoretical UTS was estimated from fiber strength and fiber volume fraction and compared with the experimental results in Fig. 9. Error bars of the experimental UTS show minimum and maximum UTS of the same specimens. Correlation between the experimental and theoretical UTS is obvious, while there is some scatter. To increase fiber volume fraction is very effective to increase UTS.

Correlation between Tensile Properties and Flexural Properties

Correlation of rough trend between tensile and flexural properties was seen. Flexural properties include compression of the specimens. It is said that compressive stress is much larger than tensile stress in SiC/SiC composites. In this study, most of PLS and flexural strength of flexural tests were larger than the results of tensile tests.

Irradiation Experiments

The specimens used in this experiment are supposed to use for irradiation experiments, HFIR 14J, rabbits, JMTR. First specimens is supposed to be irradiated at rabbits from 26 July to 21 August, 2000 at the cycle 381 and from 7 September to 1 October, 2000 at the cycle 382. Table 4 shows material properties and irradiation conditions. Each rabbit contained 4 tensile bars, 6 transthickness specimens and SiC temperature monitor as shown in Fig. 10. The specimens will be irradiated at JMTR 00M-95U. Total dose and temperature expected are 1 dpa and 800 or 1000 °C. In this capsule, in-plane tensile bars, double-notched specimens (DNS) [17] and bend bars will be contained. DNS

Table 4: Material properties and irradiation condition of rabbits cycle 381 and 382

	Fiber	Interphase	Position	Temp. (°C)	Dose (dpa) /cycle	Total dose (dpa)
FUN 1	Hi-Nicalon Type-S	Py C T1	1	380	0.8	0.8
FUN 2	Hi-Nicalon Type-S	Py C T1	1	380	0.8	1.8
FUN 5	Hi-Nicalon Type-S	Py C T2	1	380	0.8	1.8
FUN 17	Tyranno SA	Py C	2	615	1.4	2.8
FUN 21	SCS-9	Py C (1ML SiC)	2	615	1.4	2.8

will be used to evaluate interfacial shear strength.

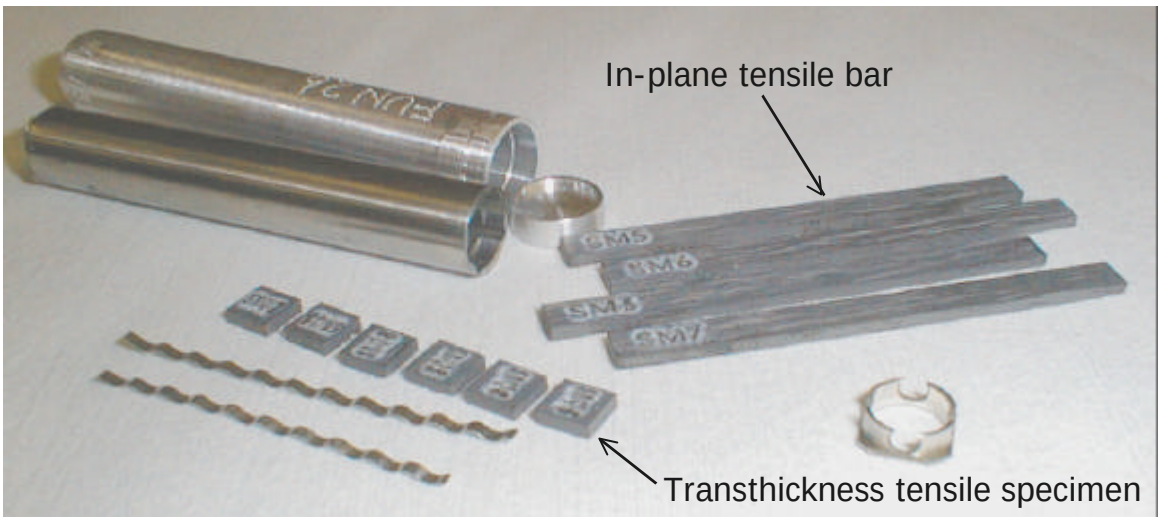

Fig. 10: Rabbit capsule and specimens to be irradiated

CONCLUSIONS

(1) SCS-9A^{TM} specimens showed superior UTS, more than 1 GPa at maximum, to the other fiber specimens. However PLS of Hi-Nicalon^{TM} type-S specimens was larger than one of SCS-9A^{TM} specimens. Tyranno^{TM} SA specimens showed brittle fracture behavior.
(2) Multiple SiC fiber coating specimens were brittle compared with the other fiber coating specimens.
(3) It was obvious that UTS depended on fiber strength and fiber volume fraction.
(4) Corresponding of rough trend between tensile and flexural properties was seen. However there were some differences in the effect of fiber coating on mechanical properties.
(5) Transthickness tensile tests were unsuccessful because of insufficient bond between fixture and epoxy. Modification of fixture surface or fixture material is required.

ACKNOWLEDGE

This work was supported by Japan-USA Program of Irradiation Test for Fusion Research (JUPITER) and by Core Research for Evolutional Science and Technology (CREST) program under the title of "R & D of Environment Conscious Multi-Functional Structural Materials for Advanced Energy Systems".

REFFERENCES

[1] P. Fenici, A.J. Frias Rebelo, R.H. Jones, A. Kohyama and L.L. Snead, J. Nucl. Mater., 258-263

(1998) 215.

[2] L.L. Snead, R.H. Jones, A. Kohyama and P. Fenici, J. Nucl. Mater., 233-237 (1996) 26-36.

[3] L.L. Snead, M.C. Osborne and K.L. More, J. Mater. Res. 10(3) (1995) 736.

[4] A. Hasegawa, G. E. Youngblood and R.H. Jones, J. Nucl. Mater., 231 (1996) 245.

[5] M.C. Osborne, C.R. Hubbard, L.L. Snead and D. Steiner, J. Nucl. Mater., 253 (1998) 67-77.

[6] G.E. Youngblood, R.H. Jones, A. Kohyama and L.L. Snead, J. Nucl. Mater., 258-263 (1998) 1551-1556.

[7] J.H.W. Simmons, Radiation Damage in Graphite, Pergamon Press, (1965).

[8] Y. Katoh, T. Hinoki, A. Kohyama, T. Shibayama and H. Takahashi, Ceram. Eng. Sci. Proc., 20 [4] (1999) 325-332.

[9] M. Takeda, A. Urano, J. Sakamoto and Y. Imai, J. Nucl. Mater., 258-263 (1998) 1594-1599.

[10] T. Ishikawa, Y. Kohtoku, K. Kumagawa, T. Yamamura and T. Nagasawa, Nature, 391 (1998) 773-775.

[11] Internet homepage of Textron systems Inc., http://www.systems.textron.com/scs9.htm.

[12] C.A. Lewinsohn, L.A. Giannuzzi, C.E. Bakis and R.E. Tressler, J. Am. Ceram. Soc., 82 [2] (1999) 407-413.

[13] L.L. Snead, M.C. Osborne, R.A. Lowden, J. Strizak, R.J. Shinavski, K.L. More, W.S. Eatherly, J. Bailey and A.M. Williams, J. Nucl. Mater., 253 (1998) 23-30.

[14] E. Lara-Curzio and M. K. Ferber, Numerical Analysis and Modeling of Composite Materials, Ed. J. W. Bull, Blackie Academic & Professional, 12 (1995) 357-399.

[15] T. Hinoki, W. Zhang, A. Kohyama, S. Sato and T. Noda, J. Nucl. Mater., 258-263 (1998) 1567-1571.

[16] J.P. Piccola, Jr., M.G. Jenkins and E. Lara-Curzio, Thermal and Mechanical Test Methods and Behavior of Continuous-Fiber Ceramic Composites, ASTM STP 1309, Edited by M.G. Jenkins, S.T. Gonczy, E. Lara-Curzio, N.E. Ashbaugh and L.P. Zawada, American Society for Testing and Materials, (1997) 3-15.

[17] E. Lara-Curzio and M. K. Ferber, Thermal and Mechanical Test Methods and Behavior of Continuous-Fiber Ceramic Composites, ASTM STP 1309, Edited by M.G. Jenkins, S.T. Gonczy, E. Lara-Curzio, N.E. Ashbaugh and L.P. Zawada, American Society for Testing and Materials, (1997) 31-48.